第 26卷 第 3期
2005年 3月
焊 接 学 报
TRANSACTIONS OF THE CHINA WELDING INSTITUTION
Vol. 26 No. 3
March 2005

钴基高温活性钎料钎焊 SiC陶瓷的接头组织及性能

谢永慧， 熊华平， 毛 唯， 程耀永
（北京航空材料研究院 焊接及锻压研究室，北京 100095）

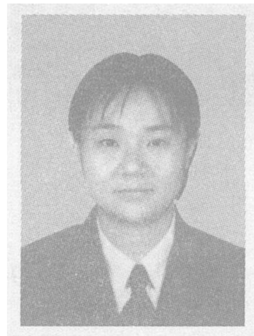
谢永慧

摘 要：采用一种钴基高温活性钎料钎焊 SiC陶瓷，研究了钎料厚度、钎焊温度对接头组织，特别是界面反应区组织以及接头室温四点抗弯强度的影响。结果表明，钎料与 SiC陶瓷的反应界面可分为富 Ni、Co，富 Cr及 富 Ti的三个区域。Ni、Co等元素在陶瓷/钎料界面强烈富集，表现出强的界面活性的特点，Cr元素次之，而 Ti元素的活性作用表现并不明显，在距陶瓷/钎料界面一定距离处形成一条富 Ti的条带。在 1 150 ℃保温 10 min的钎焊规范下，对应钎料厚度为 120 μm时获得的接头室温四点抗弯强度最高，平均达到 160 MPa。

关键词：陶瓷；界面反应；活性钎料；四点抗弯强度
中图分类号：TG425 文献标识码：A 文章编号：0253-360X(2005)03-55-03

0 序 言

SiC陶瓷由于具有良好的高温抗氧化性、耐磨性和优异的机械性能而被认为是一种很有前途的高温结构材料。SiC陶瓷的连接是其获得工程实用所需解决的关键问题之一。其中活性钎料直接钎焊法，由于钎料中含有活性元素，陶瓷表面无需预金属化，工艺简单实用而成为使用最为广泛的方法之一。为最大限度发挥陶瓷的高温性能，设计合适的高温钎料成为目前陶瓷钎焊研究的热点。

使用传统的 Ag-Cu基钎料，接头使用温度不超过 500 ℃，而含贵重金属 Au、Pd的钎料合金体系，往往依赖于钎焊前对待焊陶瓷表面预镀碳膜或金属膜以促进钎料对陶瓷的润湿，对应陶瓷自身钎焊接头的高温稳定性不超过 700 ℃[1-3]。有些研究者使用 Ni-Ti、Fe-Ti、Ti-Co钎料进行 SiC陶瓷的连接，但连接温度高达 1 623～1 823 K[4,5]。另有报道 Ni基的 Ni-20Cr-10Si钎料不含贵重金属，且对陶瓷的钎焊接头在 500～900 ℃的测试温度下强度相对于室温有所提高，但其接头室温强度偏低，另外由于钎料脆性大，钎料只能以膏状形式使用[6]。

目前已研制了一系列以钴为基，添加 Fe、Ni、Cr元素和活性元素 Ti以及少量 Si、B作为降熔元素的高温活性钎料[7]。文中采用其中的一种钎料来钎焊 SiC陶瓷，研究了钎料厚度、钎焊温度对接头组织和室温四点抗弯强度的影响。

收稿日期：2004-05-19
基金项目：国家自然科学基金资助项目（59905022）

1 试验方法

试验用陶瓷为热压烧结 SiC（烧结剂为 Al_2O_3、Y_2O_3），钎焊用钎料成分为 CoFeNi(Si, B)-(8-15)Cr-(14-21)Ti（质量分数，%），使用形式为厚度 40 μm，宽度 5 mm的箔带，熔化温度约 1 110 ℃。在真空炉中进行陶瓷的钎焊，钎焊过程中炉内热态真空度优于 5×10^{-3} Pa，升、降温速度小于 10 ℃/min。钎焊温度选择 1 150 ℃、1 180 ℃和 1 220 ℃，保温时间均为 10 min，分别添加一层、二层和三层钎料，相应钎料厚度为 40 μm、80 μm和 120 μm。金相试样沿横截面切开，磨平抛光后表面喷金，在 JSM-5600LV扫描电镜上观察接头组织的背散射电子像，并利用其附带的 LINK ISIS3000能谱仪测试陶瓷/钎料反应界面上 Ti、Si、Co、Cr、Ni等元素的面分布。弯曲性能试样接头采用对接形式，单个试样尺寸为 3 mm×4 mm×20 mm，按 GB6569-86标准试验方法进行测试。

2 试验结果及分析

2.1 接头组织形貌

图 1为在钎焊温度 1 150 ℃和 1 220 ℃下，钎料厚度分别为 40 μm和 120 μm时保温 10 min获得的 SiC陶瓷接头组织形貌。从图中可以看出，在同一钎焊温度下，钎料厚度从 40 μm增加至 120 μm，钎缝宽度显著增加，而陶瓷/钎料界面反应区宽度却有所减小。钎料厚度不变，钎焊温度提高，焊缝中的黑

色化合物相明显减少,界面反应区宽度增加。例如,钎料厚度为 120μm,钎焊温度为 1 150 ℃时在焊缝中分布着灰色的圆块状相,周围还有小的黑色条、块状相。界面反应区宽度为 15μm,紧靠焊缝有一黑色的条带,宽度约 4μm。钎焊温度提高至 1 220 ℃,焊缝中组织变得较为均匀,界面反应区增宽至 32μm,靠近焊缝的黑色条带依然存在,而 SiC陶瓷侧出现了连续的白色反应带。

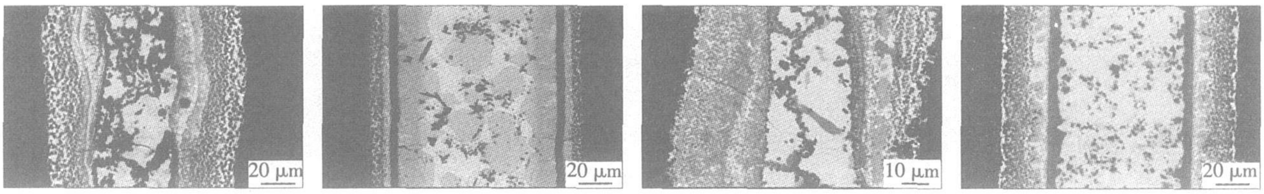

(a) 1 150 ℃×10 min,钎料厚度 40 μm
(b) 1 150 ℃×10 min,钎料厚度 120 μm
(c) 1 220 ℃×10 min,钎料厚度 40 μm
(d) 1 220 ℃×10 min,钎料厚度 120 μm

图 1 SiC陶瓷接头组织背散射电子像

Fig. 1 Back scattered microscopy of SiC bonded joint microstructure

图 2为 1 150 ℃保温 10 min,钎料厚度为 120μm时钎焊的 SiC接头界面组织及 Ti、Si、Cr、Co、Ni等元素的面分布。可以看出钎料与 SiC陶瓷发生了强烈的界面反应,反应层可分成 1、2、3三个区域。紧靠 SiC侧的 1区为白亮基体上分布着尺寸不一的黑色颗粒状化合物。元素面分布表明 1区富 Co、Ni元素,Cr元素含量较少,几乎不含 Ti元素;2区紧靠 1区,在白亮带上分布着灰块状的化合物,Cr元素明显富集,而 Ti、Co、Ni元素含量较低;3区靠近焊缝,为一条黑带,Ti元素强烈富集,而其它元素含量都很低。

从图 2看出 Ti元素的活性作用表现并不明显,

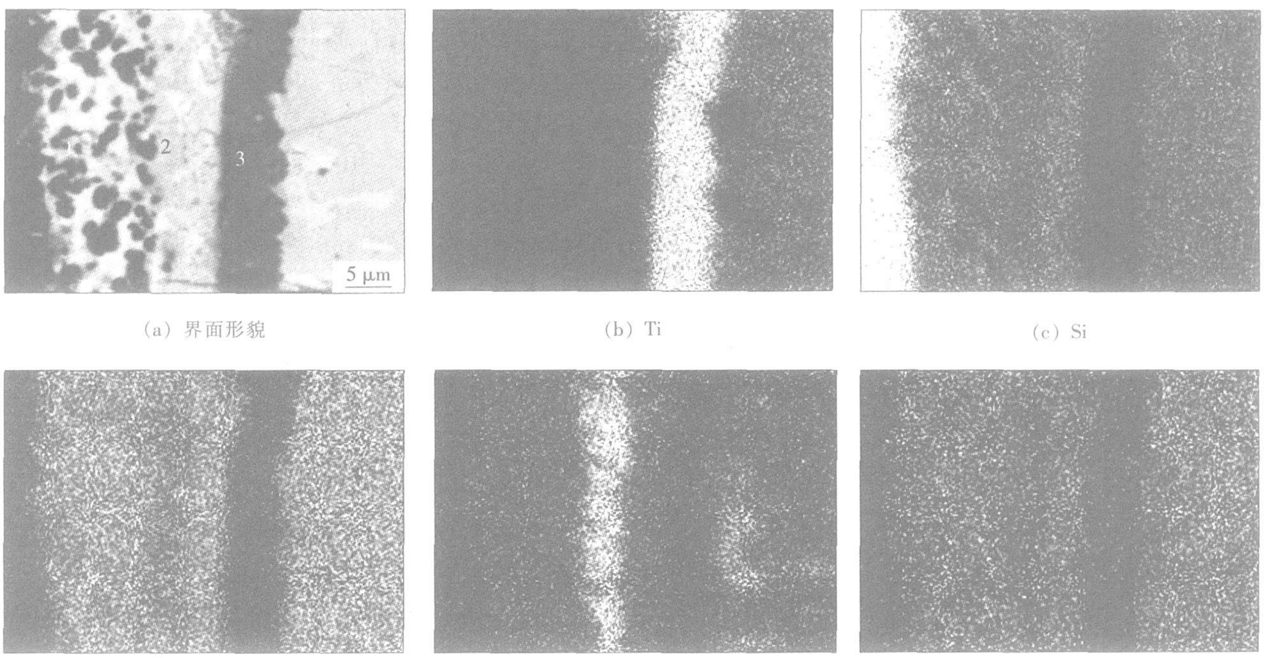

(a) 界面形貌 (b) Ti (c) Si
(d) Co (e) Cr (f) Ni

图 2 1 150 ℃×10 min钎焊接头的 SiC/钎料界面形貌及元素面分布图

Fig. 2 SiC/brazing alloy interfacial microstructure and element distribution at 1 150 ℃×10 min

未在界面富集,而是集中分布在距陶瓷/钎料界面一定深度处,Ni、Co等元素表现出强的界面活性的特点,Cr元素次之,Ti元素最低。根据文献 [8]的分析,在高温下金属 (Me)与 SiC之间可能发生如下两种类型的反应:

第一类型:Me + SiC→ 硅化物 + C (石墨)

第二类型:Me + SiC→ 硅化物 + 碳化物 + ($Me_xSi_yC_z$)

元素 Ni、Fe和 Co与 SiC之间发生的反应属第

一类型,即通过反应分别生成 Ni-Si、Fe-Si、Co-Si化合物和 C(石墨);而元素 Cr和 Ti与 SiC之间发生的反应属于第二类型,反应物为硅化物、碳化物及三元化合物的混合物。文中所用钎料成分复杂,同时含有 Ni、Fe、Co、Cr、Ti等元素,结合界面反应区的成分测试结果可知,在加热反应过程中,SiC发生分解,SiC→Si + C,钎料中的元素 Co、Ni、Fe、Cr优先向 SiC扩散,与从 SiC中分解出来的 Si原子与 C原子发生反应,生成了复杂的混合产物 1区,包括 Fe、Ni、Co的硅化物、少量 Ti、Cr的碳化物、硅化物,以及 Cr-Si-C、Ti-Si-C三元化合物和石墨相。而富 Cr的 2区除含 Fe-Si、Ni-Si、Co-Si等反应物外,还包括相当含量的 Cr-Si、Cr-C、Cr-Si-C化合物。3区的主要组成物为 TiC相。除界面连续的 TiC反应带外,在接头的钎料区还存在着分散的 TiC反应物。Si元素向接头钎料区的扩散也比较明显,钎料区的硅含量较高。

2.2 接头室温四点抗弯强度

图 3为钎焊温度、钎料厚度对接头室温平均四点抗弯强度的影响曲线。可以看出在 1 150 ℃下,钎料厚度 120 μm对应的接头强度较高,平均达到 160MPa。钎料厚度不变,钎焊温度从 1150℃升至 1 220 ℃,由于紧靠 SiC陶瓷的复杂硅化物层增厚使接头强度下降。而当钎料厚度为 40 μm时,钎焊温度升高,焊缝中的化合物相减少,组织更为均匀,接头强度反而提高。在同一钎焊温度下,钎料厚度对接头强度的影响也较复杂,钎焊温度较低时,钎料厚度增加,由于元素扩散距离增大,界面反应区宽度下降,接头强度提高。在较高的钎焊温度下,钎料厚度增加,在紧靠 SiC陶瓷出现了连续的复杂化合物条带,显著降低了接头的强度。

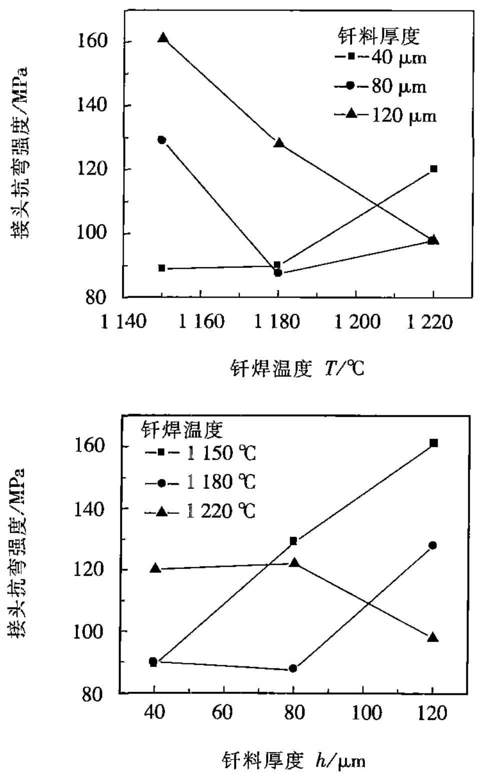

图 3　钎焊温度、钎料厚度对接头室温四点抗弯强度的影响曲线

Fig. 3　Effect of brazing temperature and brazing alloy thickness on joint four-point bending strength

3　结　　论

(1) 钴基活性钎料钎焊 SiC陶瓷的接头界面可分为富 Ni、Co、富 Cr及 富 Ti的三个区。

(2) 钎料中的 Ni、Co元素表现出强的界面活性特点,在陶瓷/钎料界面富集,而 Ti元素的活性作用表现并不明显,集中分布在距陶瓷/钎料界面一定距离处。

(3) 在 1 150 ℃×10min的钎焊规范下,相应钎料厚度 120 μm时钎焊接头的室温四点抗弯强度最高,平均达到 160MPa。

参考文献:

[1]　Okamura H. Brazing ceramics and metals[J]. Welding International, 1993, 7(3): 236-242.

[2]　Kang S, Kim H J. Design of high temperature brazing alloys for ceramic-metal joints[J]. Welding Journal, 1995, 74(9): 289-295.

[3]　Tillmann W, Lugscheider E, Schlimbach K, et al. Heat resistant active brazing of silicon nitride[J]. Welding Journal, 1998, 77(3): 103-109.

[4]　Fukai T, Liu Yuli, Naka M. Diffusion bonding of sic ceramic by Fe-Ti alloy[J]. Transactions of the China Welding Institution, 1998, 19(2): 93-96.
深井卓,刘玉莉,奈贺正明. 用 Fe-Ti合金钎焊连接 SiC陶瓷[J]. 焊接学报, 1998, 19(2): 93-96.

[5]　刘玉莉,冯吉才,奈贺正明. 用 Ti-Co合金扩散连接 SiC陶瓷[J]. 哈尔滨工业大学学报, 1998, 30(6): 61-64.

[6]　Ali Mohammad Hadian, Robin A L Drew. Strength and microstructure of silicon nitride ceramics brazed with nickel-chromium-silicon alloys[J]. J Am. Ceram Soc, 1996, 79(3): 659-665.

[7]　熊华平,毛　唯,程耀永,等. 几种钴基高温钎料对 SiC陶瓷的润湿与界面结合[J]. 金属学报, 2001, 37(9): 991-996.

[8]　Park J S, Landry K, Prepezko J H. Kinetic control of silicon carbide/metal reactions[J]. Materials Science and Engineering, 1999, A259(2): 279-286.

作者简介:谢永慧,女,1973年生,博士。主要从事高温材料的真空钎焊工艺研究,已发表论文 10余篇。

Email: yonghui-cn@sina.com

sing the technology of narrow band filter, which is used to overcome the influence of strong arc light. Meanwhile, the aluminum alloy characteristic of the MIG welding pool is analyzed. In order to overcome the disadvantages of traditional welding pool image processing method, the morphological operators is used to process the aluminum alloy MIG welding pool. The method can effectively wipe off noise and ‘cathode pulverization’ area in image. Experiments show that the method is effective and feasible, and it can provide reliable information for the real-time control of aluminum alloy MIG welding process.

Key words: aluminum alloy; metal inert-gas welding; morphology; vision sensing system

J-R resistance curves of welded joints for X56 pipeline steel DENG Cai-yan, ZHANG Yu-feng, HUO Li-xing (School of Material Science and Engineering, Tianjin University, Tianjin 300072, China). p41-44

Abstract: In accordance with the BS7448, fracture toughness test standard, J-Resistance curve tests were conducted with the multiple specimen at -5 ℃ in welded joints of X56 pipeline steel. According to the standard, the specimen with fatigue precrack is a standard three point bending shape that has a rectangular section of $B \times 2B$ (B: specimen thickness) and notch orientation of thickness direction. And then based on the double P-V (P: load, V: displacement) curves of each weld metal and HAZ (heat affected zone) specimen obtained from the two notch opening displacement, the load-line displacement and the value of J were calculated. Finally, the paper determined the best fit curve through the valid data points, and got $J_{0.2}$ at all fatigue crack tips locating in HAZ by analyzing the fracture section of HAZ specimen, so the test results of HAZ are reliable. The BS 7448 Part 4, the standard on metallic materials, was applied to establish J-R curves of welded joints. Test results provide reliable evidence for engineering critical assessment.

Key words: X56 pipeline steel; welded joint; J integral; resistance curve

Principle of rotating transfer undergoing longitudinal magnetic field control CHEN Shu-jun[1,2], WANG Jun[3], WANG Hui-xia[3], LIU Zhen-yang[2], YIN Shu-yan[2], Bai Shao-jun[2] (1. National Key Laboratory of Advanced Welding Production Technology, Harbin Institute of Technology, Harbin 150001, China; 2. College of Mechanical Engineering & Applied Electronics Technology, Beijing University of Technology, Beijing 100022, China; 3. College of Material Science and Engineering, Hebei University of Science and Technology, Shijiazhuang 050054, China). p45-49, 54

Abstract: The dynamic process of rotating transfer undergoing the longitudinal magnetic field control is discussed, and the formation of circum-current is analyzed because of the rotating of the liquid streaming. The process of rotating transfer is affected by the interaction of the circum-current and the additional longitudinal magnetic field. The experimental results show that the process of rotating transfer can be controlled by the additional longitudinal magnetic field. Under the shielding gas of 80% Ar +20% CO_2, a stable and better controlled rotating transfer is realized with the wire feed speed of 45 m/min. Thus the melting efficiency of the welding materials increases obviously. In this case, a new metal active-gas welding process with higher performance and less cost is realized under the condition of the continuous and high current with the common shielding gas free of helium.

Key words: longitudinal magnetic field; high performance metal active-gas welding; rotating transfer

Interfacial characteristics of diamond brazed by high-frequency induction MA Bo-jiang, XU Hong-jun, FU Yu-can, XIAO Bing, XU Jiu-hua (College of Mechanical and Electrical Engineering, Nanjing University of Aeronautics & Astronautics, Nanjing 210016, China). p50-54

Abstract: The interfacial characteristics of the Ti-coated diamonds and uncoated diamonds was investigated. The interfaces were brazed by high-frequency induction with two kinds of Ni-Cr alloys on the same conditions. The grains brazed by high-frequency induction were immerged into the mixed acids for several hours and then rinsed with acetone. The interfacial characteristics of the grains were studied with scanning electron microscope, energy dispersion spectrometer and X-ray diffraction. The results show that the composition and the shape of carbides of the brazed diamond grains are different when different solders were used to braze diamonds with or without Ti coatings. The Cr-carbides of brazed Ti-coated diamond grains are normally and compactly formed, whereas, the Cr-carbides on the surface of brazed uncoated diamond are tangentially and loosely formed. The abrasive experiment indicates that the bond strengths between the carbide and the diamonds are also different with different carbides.

Key words: induction brazing; diamond; interfacial characteristics; bonding strength

Microstructure and mechanical propertites of SiC joint brazed with heat resistant active brazing alloys XIE Yong-hui, XIONG Hua-ping, MAO Wei, CHENG Yao-yong (Beijing Institute of Aeronautical Materials, Beijing 100095, China). p55-57

Abstract: SiC ceramics were bonded with a cobalt based heat resistant active brazing alloy. The effect of brazing alloy thickness and brazing temperatures on the joint microstructurs and four-point bending strength was studied. Results show that the SiC/brazing alloy interface could be divided into three zones, one rich in Ni and Co, one rich in Cr and another rich in Ti. Ni and Co elements integrated at the interface, while the active Ti element distributed in the area with some distance from the interface. When the joint was brazed at 1150℃ for 10 min and the thickness of brazing alloy is 120 μm, the four-point bending strength of joints reached the maximum with an average value of 160 MPa.

Key words: ceramic; interfacial reaction; active brazing alloys; four-point bending strength

An recognition algorithm on underwater welding seam tracking